Proceedings of Symposium on Ultrasonic Electronics, Vol. 31 (2010) pp. 467-468
6-8 December, 2010

Effects of elastic anisotropy on acoustic-wave rectification
音響波整流における弾性的異方性の効果

Takahiro Murai, Yukihiro Tanaka† and Norihiko Nishiguchi (Department of Applied Physics, Hokkaido University)
村井剛博，田中之博†，西口規彦 (北大院工)

1. Introduction

Rectification of acoustic waves or heat flow has recently attracted a great deal of attention from a theoretical and practical point of view[1-6]. The rectification means that acoustic energy flows more easily in one direction than in the other, forming a regulator for acoustic waves in solids. Liang *et al.* recently proposed a mechanism of acoustic wave rectification utilizing phonon mode conversions owing to nonlinear effects in the constituent materials[6], but it is difficult to actually fabricate such a device since suitable materials having extremely strong elastic nonlinearity are not available.

In a previous work[7], we proposed a simpler model of acoustic-wave rectifier without relying on the nonlinearity; triangular holes align with the same separation in the elastically-isotropic substrate, as shown in Fig. 1(a).We confirmed numerically that the system works for rectifying bulk acoustic waves; the acoustic wave propagating in (I)-direction is transmitted beyond the scatterers more than that propagating in (II)-direction.

Most crystalline materials have elastic anisotropy. For example, crystalline copper has large elastic anisotropy; the anisotropy factor A defined by $A = 2C_{44}/(C_{11}-C_{12})$ becomes $A = 3.2 > 1$ [8], where $\{C_{ij}\}$ are the stiffness tensor elements in cubic crystals. The slowness curve in the (001) plane is illustrated in Fig. 1(b), showing the group and phase velocities of an acoustic wave are not generally collinear. Then one expects that the phenomenon affects the rectification effects on the phonon propagation, but the effects are not easy to speculate. The purpose of this work is to elucidate the effects of elastic anisotropy on the rectification of acoustic waves, by means of numerical simulations.

2. Model and methodology

The acoustic-wave rectifier considered here is composed of crystalline copper with aligned isosceles-triangular holes with the summit angle α in the y direction as shown in Fig.1(a). Neighboring triangular holes are separated by the same distance as the base length, a so the periodicity of the array is $D = 2a$. The axes of the holes are set in the z direction corresponding to the crystal axis [001] of cubic symmetry. The substrate is assumed to expand in the z direction infinitely, so that the system is homogeneous in the z direction.

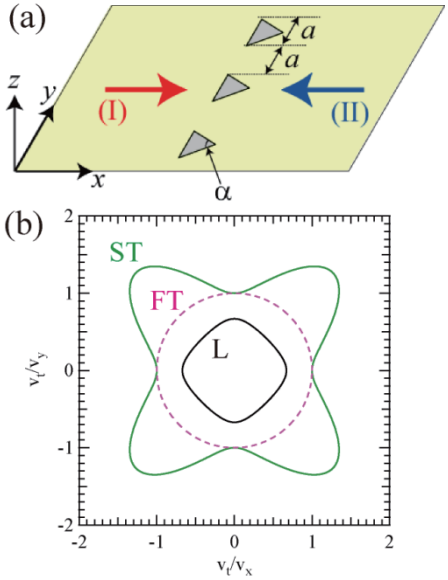

Fig. 1(a) Acoustic-wave rectifier proposed. Thick arrows indicate the direction of incident waves. (b) Slowness curve of copper in the (001) plane. The green and black solid lines represent slow-transverse (ST) and quasi-longitudinal (L) waves, respectively, which couple each other in arbitrary angle in the (001) plane. And a dashed pink line indicates fast-transverse (FT) waves whose polarization is along the [001] direction independently. v_t is the velocity of transverse waves in the [100] direction.

The equations of motion governing the displacement field $u_i(\mathbf{r},t)$ and the stress tensor $\sigma_{ij}(\mathbf{r},t)$ are given by

$$\rho(\mathbf{r})\ddot{u}_i(\mathbf{r},t) = \partial_j \sigma_{ij}(\mathbf{r},t) \quad (i=1,2,3), \qquad (1)$$

$$\sigma_{ij}(\mathbf{r},t) = c_{ijkl}(\mathbf{r})\partial_l u_k(\mathbf{r},t) \quad (i,j=1,2,3), \qquad (2)$$

where $\mathbf{r} = (x,y)$, and $\rho(\mathbf{r})$ and $c_{ijkl}(\mathbf{r})$ are the position-dependent mass density and stiffness tensor of the substrate, respectively. The summation convention over repeated indices is assumed in the equation.

To specify the effects of the anisotropy on the acoustic-wave rectifier, we focus our attention on the mixed modes propagating on the (001) plane,

e-mail : yuki@eng.hokudai.ac.jp

which consist of quasi-longitudinal (L) and slow-transverse (ST) waves as shown in Fig.1(b), considering that it is obvious from Fig. 1(b) that there is no nonlinear effect on propagation of the fast-transverse (FT) waves, and FT mode waves do not mix with other modes.

We numerically solve these equations using finite-difference time-domain (FDTD) method [9] and can obtain the time evolutions of the displacement field and the stress tensors at each spatial grid, and then we can calculate $\hat{u}_i(\mathbf{r},\omega)$ and $\hat{\sigma}_{ij}(\mathbf{r},\omega)$ in frequency domains using Fourier transform. Using them, we can evaluate the acoustic energy flow passing through a position x along the x direction in the frequency domain;

$$\hat{J}_x(x,\omega) = -4\pi \int \mathrm{Im}\left[\omega \hat{u}_j(\mathbf{r},\omega)\hat{\sigma}^*_{jx}(\mathbf{r},\omega)\right] dy \,. \quad (3)$$

Hence we define the transmission rate $T(\omega)$ by the ratio of the x component of the acoustic Poynting vector $\hat{J}_x(x_D,\omega)$ to that in the absence of holes $\hat{J}^0_x(x_D,\omega)$;

$$T(\omega) = \frac{\hat{J}_x(x_D,\omega)}{\hat{J}^0_x(x_D,\omega)}, \quad (4)$$

where x_D represents the detecting position which is on the right side of the triangular holes for case(I) (whose incident wave goes toward the bases) and on the left side for case(II) (whose incident wave goes toward the summits) .

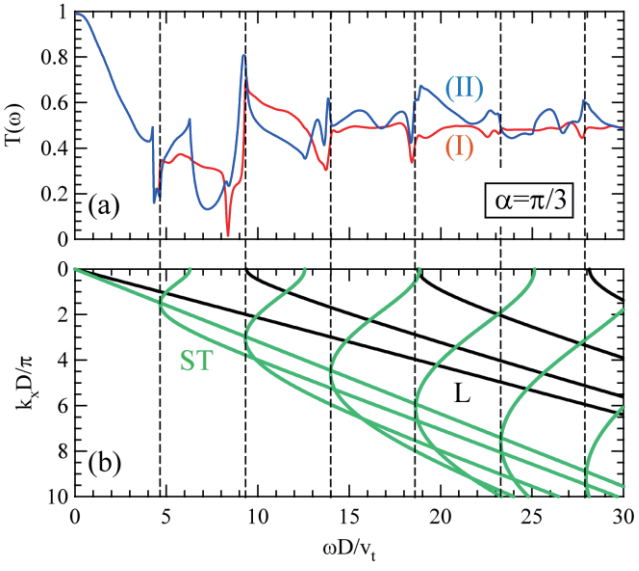

Fig. 2(a) Transmission rates versus frequency for the case with $\alpha = \pi/3$ (forming an equilateral triangular hole). Red and blue lines indicate case (I) and (II), respectively. The incident wave is a longitudinal one. (b) Dispersion relations of mixed modes along the x direction within empty-lattice approximation. Black and green lines represent longitudinal (L) and slow-transverse (ST) modes, respectively. Dashed lines indicate the frequencies of local minima in the ST curves.

3. Numerical Results

Exciting a longitudinal wave-packet with gaussian distribution in frequency propagating in the x (or [100]) direction, we investigate the transmission of the waves. The central frequency is $\omega D/v_t = 14$ and its width $\Delta\omega D/v_t = 9$ so that the spectra cover the entire frequency region of interest.

Fig.2(a) shows the transmission rates versus frequency for the case with $\alpha = \pi/3$ (forming an equilateral triangular hole). The transmissions of cases (I) and (II) coincide in the low frequency region. On the other hand, there is disagreement in magnitude between (I) and (II) above a threshold frequency (as we will discuss below). In contrast to the rectifier made of the isotropic material, it is found that the transmission rates of the case (I) and (II) are comparable, manifesting that the elastic anisotropy suppresses performance of rectification effects.

Finally, we plot in Fig.2(b) the dispersion relation of mixed modes along the x direction within empty-lattice approximation in order to understand the singular behaviors in the transmission rates. We can see sub-band structures for ST and L modes, which correspond to different reciprocal lattice vector in the y direction. The singular behaviors occur when the curves of ST modes have local minima due to elastic anisotropy, where mode conversions from L modes to ST ones or vice versa are enhanced because of the large density of states of ST modes.

References

1. M. Terraneo, M. Peyrard and G. Casati, Phys. Rev. Lett. **88**, 094302 (2002).
2. Baowen Li and Jiao Wang, Phys. Rev. Lett. **91**,044301 (2003).
3. Baowen Li, Lei Wang and G. Casati, Phys. Rev. Lett. **93**, 184301 (2004).
4. C. W. Chang, D. Okawa, A. Majumdar and A. Zettl, Science **314**, 1121-1124 (2006).
5. N. A. Roberts and D. G. Walker, ITherm08, Orlando, FL,USA (2008).
6. B. Liang, B. Yuan and J-C. Cheng, Phys. Rev. Lett. **103**, 104301 (2009).
7. S. Shirota, Ramya Krishnan, Y. Tanaka and N. Nishiguchi, Jpn. J. Appl. Phys. **46**, L1025-L1027 (2007).
8. We use the elastic constants (in units of 10^{11} dyn/cm^2) and the mass density (in units of g/cm^3) $C_{11} = 16.8$, $C_{12} = 12.1$, $C_{44} = 7.54$ and $\rho = 8.92$ for copper, respectively.
9. In our simulation the grid size used is $\Delta x = \Delta y = D/100$, and the time interval is $\Delta t = 5.0\times10^{-4} D/v_t$.